Talanta 284 (2025) 127211

Contents lists available at ScienceDirect

Talanta

journal homepage: www.elsevier.com/locate/talanta

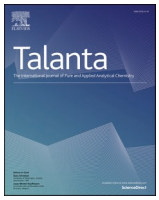

Metabolomic study for the identification of symptomatic carotid plaque biomarkers

Marina Botello-Marabotto [a,b,c], Emma Plana [d,e,*], M. Carmen Martínez-Bisbal [a,b,c,f,**], Pilar Medina [d], Andrea Bernardos [b,c,g], Ramón Martínez-Máñez [a,b,c,g,h,1], Manuel Miralles [d,e,i,1]

[a] Unidad Mixta de Investigación en Nanomedicina y Sensores, Instituto de Investigación Sanitaria La Fe (IISLAFE), Universitat Politècnica de València, Valencia, Spain
[b] Instituto Interuniversitario de Investigación de Reconocimiento Molecular y Desarrollo Tecnológico (IDM), Universitat Politècnica de València - Universitat de València, Valencia, Spain
[c] CIBER de Bioingeniería, Biomateriales y Nanomedicina, Instituto de Salud Carlos III, Spain
[d] Grupo Acreditado de Hemostasia, Trombosis, Arteriosclerosis y Biología Vascular, Instituto de Investigación Sanitaria La Fe (IISLAFE), Valencia, Spain
[e] Servicio de Angiología y Cirugía Vascular, Hospital Universitario y Politécnico La Fe, Valencia, Spain
[f] Departamento de Química Física, Universitat de València, Valencia, Spain
[g] Unidad Mixta UPV-CIPF de Investigación en Mecanismos de Enfermedades y Nanomedicina, Universitat Politècnica de València, Centro de Investigación Príncipe Felipe, Valencia, Spain
[h] Departamento de Química, Universitat Politècnica de València, Valencia, Spain
[i] Departamento de Cirugía, Facultad de Medicina, Universitat de València, Valencia, Spain

ARTICLE INFO

Keywords:
Atherosclerosis
Vulnerable plaque
Metabolomics
^{1}H NMR spectroscopy
Biomarkers

ABSTRACT

Carotid artery stenosis is mainly produced due to the progressive accumulation of atherosclerotic plaque in the vascular wall. The atherosclerotic plaque is characterized by the accumulation of lipids, low density proteins, expression of chemokines and adhesion molecules, and migration of monocytes and lymphocytes into the plaque. Its rupture can produce stroke, but embolic propensity depends principally on the composition and vulnerability of plaque rather than the severity of stenosis. It is important, then, to ascertain which patients with carotid artery stenosis have a greater risk of developing neurological symptomatology. Here, we present a metabolomic study by using nuclear magnetic resonance (NMR) spectroscopy in atheroma plaque and serum samples from patients with recently symptomatic and asymptomatic carotid stenosis to search for metabolites that could be used as biomarkers associated with plaque vulnerability and subsequent risk of rupture. Thirty-eight atheromatous plaque samples (24 asymptomatic patients and 14 symptomatic) and 70 serum samples (43 asymptomatic and 27 symptomatic) were studied by NMR spectroscopy. The data were analysed using multivariate statistics (PLS-DA) to determine a model to discriminate between symptomatic and asymptomatic samples (atheroma plaques and sera). The calculated PLS-DA models showed a 100 % sensitivity and a 96.6 % specificity for the cross validation to discriminate between symptomatic and asymptomatic plaques, and 88.37 % sensitivity and 77.78 % specificity when serum samples were analysed. According to the results of our multivariate and univariate analysis, the most discriminative metabolites for plaque vulnerability were threonine in serum samples, and glutamate in plaque samples. Also, an analysis of the main metabolic pathways involved in plaque vulnerability revealed that D-glutamine and D-glutamate metabolism, and phenylalanine, tyrosine, and tryptophan biosynthesis were the most affected pathways in plaque and serum, respectively.

* Corresponding author. Grupo acreditado de Hemostasia, Trombosis, Arteriosclerosis y Biología Vascular, Instituto de Investigación Sanitaria La Fe (IISLAFE), Av. Fernando Abril Martorell, 106 Torre A. 46026 Valencia, Spain.
** Corresponding author. Departamento de Química Física, Universitat de València, C/ Doctor Moliner, 50, 46100 Burjassot, Valencia, Spain.
E-mail addresses: emma_plana@iislafe.es (E. Plana), carmen.martinez-bisbal@uv.es (M.C. Martínez-Bisbal).
[1] Equal last authors.

https://doi.org/10.1016/j.talanta.2024.127211
Received 8 May 2024; Received in revised form 30 October 2024; Accepted 11 November 2024
Available online 12 November 2024

1. Introduction

Stroke and myocardial infarction are still among the leading causes of death worldwide [1], being the development of atherosclerosis the underlying cause in most cases [2]. Based on its histological appearance and physiopathology, atherosclerosis can be considered a chronic inflammatory disease of the circulatory system [3]. It usually begins with impairment of the molecular activity of the intima layer or endothelial dysfunction, allowing the entry of macromolecules such as low density lipoproteins (LDL) into the subendothelial layer, particularly in turbulent blood flow areas. This leads to an inflammatory reaction, with LDL becoming oxidized (ox-LDL). These particles develop a chemoattraction and recruitment of monocytes and lymphocytes from the bloodstream coming inside the vessel wall. Ox-LDL particles are subsequently phagocyted and internalized by macrophages and transformed into foam cells, which are highly stimulated to produce inflammatory cytokines. Ultimately, this inflammatory environment, expression of cytokines, and growth factors result in vascular smooth muscle cell (VSMC) migration from the *media* towards the *intima*, changing their phenotype and producing extracellular matrix proteins, including collagen, as well as new waves of cytokines and growing factors. This process leads to the formation of a fibrous cap surrounding a lipid core of merging LDL particles released from apoptotic foam cells and the constitution of the atheroma plaque. The evolution of these plaques can lead to either a stable or unstable situation, primarily depending on the integrity and thickness of the fibrous cap [4].

The most clinically significant consequence of atherosclerosis plaques is the impairment of blood flow to the downstream tissues and organs, mainly due to the diameter reduction or stenosis of the vessel. Clot formation at this point may block blood flow, leading to a stroke if the occlusion is produced in the carotid artery or to myocardial infarction if it is produced in the coronary artery. The formation of thrombus is produced by the rupture or erosion of the plaque and the release of prothrombotic factors into the bloodstream. Previous to the rupture of the plaque, the fibrous cap may become thin and unstable, which is known as vulnerable plaque [5]. The reasons why the plaque can become vulnerable and rupture remain unclear.

In this context, the identification of biomarkers of plaque vulnerability would be of utmost clinical value as it could help to determine for which patients an intervention would be required to prevent clinical symptomatology.

Metabolomics has been explored as a tool for the search of biomarkers in different clinical scenarios such as cancer, inborn errors of metabolism, diabetes, infection, glaucoma, or Alzheimer's disease, among many others [6–12]. Actually, metabolomics is the omic that encloses more information to determine the cause of the pathologic problem. That is because a concrete metabolome is produced due to the combination of genetic and environmental factors, among others, so it provides broader information about the molecular features of the phenotype than any other omics science [13]. There are two main techniques to ascertain the metabolome: mass spectrometry (MS) and nuclear magnetic resonance (NMR) spectroscopy. NMR spectroscopy is a robust and reproducible technique that allows the determination of the metabolic composition of any sample (blood derivatives, cerebrospinal fluid, culture cells and media, urine, tears, tissue, etc.) without destroying it. In addition, the acquisition of NMR spectra requires simple preparation procedures and only a small amount of sample [14]. Furthermore, NMR spectroscopy allows the study of intact tissue samples through high-resolution magic angle spinning (HRMAS) without the need for extracts [15]. This opens the possibility to study samples of lower size/weight [15,16] and also enables the performance of quantitative studies [17].

In the context of atherosclerosis diagnosis and research, previous metabolomic studies for the identification of biomarkers have been performed using NMR spectroscopy. For instance, Wurtz et al. [18] performed an NMR spectroscopy study for the identification of subclinical biomarkers of atherosclerosis in plasma and found docosahexaenoic acid, glutamine, and tyrosine as potential biomarkers of atherosclerosis progression. Vorkas et al. [19] studied the metabolome composition of atheroma plaque by ultra-high performance liquid chromatography mass spectrometry (UHPLC–MS), and they found changes in the levels of acylcarnitine and phosphatidylethanolamine-ceramides. Tomas et al. [20] studied by MS the presence of biomarkers of vulnerability in carotid plaque samples. These authors found that the metabolite profile of the carotid plaques correlated with the histological analysis of the plaques in the assessment of their stability. In high risk plaques, there was increased glycolysis and amino acid metabolism and decreased fatty acid oxidation. However, previous studies do not offer a leap in the understanding of the causes leading to the development of a high-risk plaque, and a set of biomarkers that could be explored as a prognostic tool for plaque instability associated with neurological symptomatology has not yet been identified.

Aimed for this context, we have performed a metabolomic analysis of atheroma plaque and serum from patients with symptomatic and asymptomatic carotid stenosis, using NMR spectroscopy for the search of new molecules and circulating markers related to plaque vulnerability and risk of stroke in patients with carotid stenosis. These metabolites could be used as biomarkers to determine plaque vulnerability and risk of rupture.

2. Materials and methods

2.1. Patients selection

This is a case-control study, where subjects were classified as recently symptomatic patients (case) and asymptomatic patients (control). Symptomatic patients were considered when transient ischaemic attack, *amaurosis fugax*, or stroke with ischaemic origin occurred at most 3 weeks before surgery. Asymptomatic patients were subjects with severe carotid stenosis (>70 %) without neurological symptomatology submitted for carotid endarterectomy on the basis of international guidelines. The primary inclusion criteria were being an adult (over 18 years of age) and providing written informed consent. Exclusion criteria included being over 90 years of age, having terminal malignancies, and being human immunodeficiency virus positive. Patients were recruited by the Angiology and Vascular Surgery Service from the Hospital Universitario y Politécnico La Fe. Cases were enrolled consecutively, and sex- and age-matched controls were selected from an extensive biobank collection. The present study was performed according to the declaration of Helsinki and was approved by the ethical committee of the Medical Research Institute Hospital La Fe (references 2019-094-1 and 2020-189-1_PI20/01171). Samples and data from subjects included in this study were managed and provided by Biobank La Fe (PT17/0015/0043) after approval by the scientific and ethical committees. All participants agreed to donate samples to biobank and gave written informed consent.

2.2. Sample collection

Blood samples were obtained during surgery in a clot activator tube, centrifuged at 1811 g for 30 min at 4 °C within 3h after collection to separate the serum fraction, which was distributed in 300–500 μl aliquots and stored at −80 °C until used.

Atheromatous plaque samples were obtained during endarterectomy procedure according to standardized surgical protocols in the Angiology and Vascular Surgery Service from Hospital Universitario y Politécnico La Fe. Samples were rinsed with phosphate buffered saline (PBS), snap frozen in liquid nitrogen, and stored at −80 °C until use. A fragment of 0.3 cm from the most occluded zone was used for NMR analysis.

Table 1
Clinical data of patients participating in the study.

	Plaque		Serum	
	Symptomatic (n = 14)	Asymptomatic (n = 24)	Symptomatic (n = 27)	Asymptomatic (n = 43)
Age, mean (range)	70.4 (60–83)	69.4 (50–81)	68.6 (44–83)	68.8 (50–81)
Sex, male/female	13/1	21/3	24/3	38/5
Hypertension (%)	92.85	70.83	80.76	76.74
Diabetes Mellitus (%)	50	50	50	39.53
Dyslipidemia (%)	64.28	62.5	61.54	69.76
Smoking Habits [a]	4/1/9/0	7/5/12/0	6/3/17/1	17/7/19/0
Alcohol use [b]	1/13/0	2/21/1	1/26/0	5/36/2
Cannabis use [c]	0/14	0/24	1/26	0/43
CRF [d] **(%)**	7.14	12.50	7.41	16.28
COPD [d] **(%)**	21.43	8.69	18.52	19.05
Heart Diseases [e] **(%)**	21.43	39.13	22.22	50.00
Previous TIA/Stroke [f] **(%)**	14.29	8.69	18.52	14.29
Malignancies (%)	14.29	19.05	18.52	10.26
Other Vascular Diseases [g] **(%)**	21.43	66.67	18.52	50.00
Antihypertensive Drugs (%)	78.57	62.50	74.07	76.74
Lipid-lowering Drugs (%)	64.29	79.17	66.67	81.39
Antidiabetic Drugs (%)	42.86	50.00	40.74	32.56
Antidepressant or Sedatives (%)	7.14	33.33	22.22	23.26
Anticoagulant Drugs (%)	15.38	26.09	11.54	29.27
Anti-platelet Drugs (%)	78.57	83.33	66.67	79.07
BMI [d]**, mean (range)**	28.45 (24.03–33.20)	24.69 (18.52–30.10)	28.27 (21.33–33.51)	26.44 (18.52–35.16)

[a] Smoking habits yes/no/ex/not available.
[b] Alcohol use yes/no/ex.
[c] Cannabis use yes/no.
[d] CRF: chronic renal failure; COPD: chronic obstructive pulmonary disease; BMI: body mass index.
[e] Ischemic heart disease, heart attack, angina.
[f] Previous transient ischemic attack (TIA) or stroke, more than 1 month before surgery.
[g] Thrombosis, aneurysms, limb ischemia.

2.3. Sample preparation

The 38 collected atherosclerotic plaques (14 from symptomatic patients and 24 from asymptomatic ones) were analysed by HRMAS NMR spectroscopy. For this purpose, tissue samples (10 ± 5 mg) were introduced in a 4 mm disposable micro-rotor with 10 μl of D_2O, with sodium 3-(trimethylsilyl)-1-propanesulfonic acid d_6 sodium salt (DSS-d_6) 5 mM as an internal standard for chemical shift referencing.

In a parallel substudy, 70 serum samples (35 of them paired with the atheroma plaque samples studied by HRMAS) were analysed by NMR spectroscopy. The samples were prepared following the protocol described by Beckonert et al. [21] Briefly, 250 μl of the serum sample were introduced in 5 mm NMR tubes and 250 μl of phosphate buffer was added. Phosphate buffer contained deuterated water (20 % v/v) and DSS 1 mM as an internal standard for chemical shift referencing.

2.4. NMR spectra acquisition and processing

The atheroma plaque experiments were carried out in a Bruker Avance II 500 MHz equipped with an HRMAS probe (Bruker BioSpin). Noesy sequence was used for the acquisition of the 1D ^{1}H NMR spectra of the plaques. 256 scans and a spectral width of 14 ppm were acquired. NMR spectra from the serum samples were acquired in the same 500 MHz spectrometer equipped with a TXI probe (Príncipe Felipe Research Center Foundation (CIPF) NMR facility). In each set of samples, atheroma plaques and sera were measured randomly to avoid any bias due to sample order. Due to the robustness and reproducibility of NMR spectroscopy, no technical repetitions were necessary, and each sample was measured only once. Noesy experiments were acquired, with 128 repetitions and a spectral width of 30 ppm. In both types of samples, 2D homo (^{1}H–^{1}H) and heteronuclear (^{1}H–^{13}C) spectra were acquired to guarantee the assignment of the metabolites in the spectra. The temperature of the probes for both tissues and sera was set to 278 K (5 °C).

Once obtained, the 1D spectra were transformed and post-processed with the *TopSpin 4.0.7* software (Bruker BioSpin Corporation). The phase and baseline of the spectra were corrected, and the chemical shift was calibrated according to the DSS CH_3 signal at 0.0 ppm. The Human Metabolome Database (HMDB) [22], Chenomx NMR Profiler [23], and previously published bibliography [15] were used for metabolite identification, by comparing the spectra profile in the samples with the spectra of standards in these resources.

Meaningful signals underwent deconvolution using *AMIX 4.0.2* software (Bruker BioSpin Corporation), excluding the water suppression signal (4.5–5.0 ppm) and the signals at ppm lower than 0.5 ppm and higher than 8.5 ppm. Then, a mixed Gaussian/Lorentzian variable function was applied for the deconvolution of these signals. Later on, integrals were obtained for all spectra in atheroma plaque tissue and serum samples. For serum samples, relative quantification was based on the integration of the signal divided by the sum of the integrals of all the signals in the spectrum. Normalization was done for the atheroma plaque samples according to their weight.

2.5. Multivariate statistical analysis

Multivariate statistical analysis was performed using the *PLS_Toolbox Solo 9.3* (2024) software (Eigenvector Research, Inc., Manson, WA, USA). The same procedures were followed with the data from the tissue and from the serum samples. Principal Component Analyses (PCA) were performed in both data sets, atheroma plaques and serum samples, to explore any potential clustering by sex of patients or by the symptomatology.

Before the model calculation, a variable reduction was performed in order to simplify the data set. The variables included in the model were selected using Genetic Algorithms (GA). GA is a common machine learning technique based on the process of natural selection that has been proven to be helpful in feature selection processes [24]. Fifty maximum generations, PLS regression with 10 latent variables, and random cross-validation (CV) with autoscaling and normalization by sum of the data were applied for variable selection.

After variable selection, partial least squares-discriminant analysis

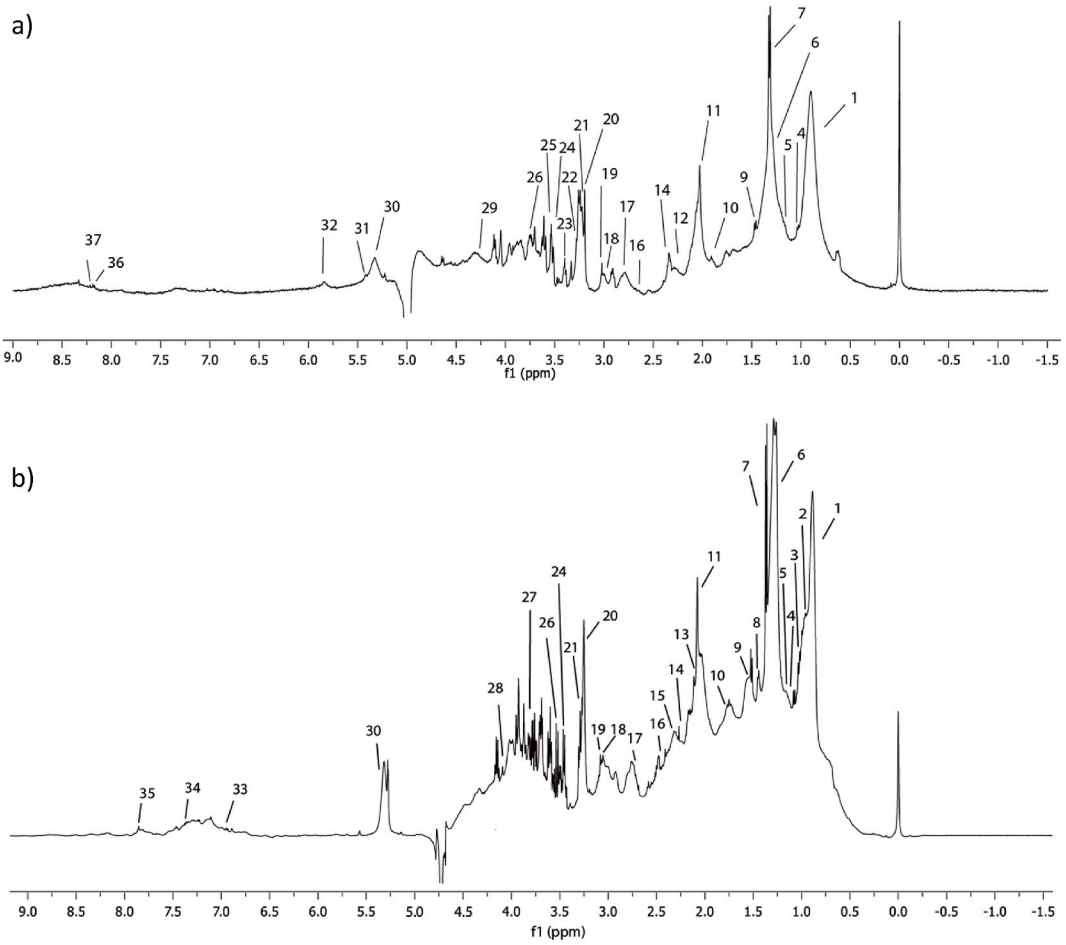

Fig. 1. Annotations of the metabolites present in the samples. a) Representative spectrum of tissue samples from atherosclerotic plaques. b) Representative spectrum of serum samples from patients with atherosclerosis. 1. Fatty Acids (–CH_2–CH_3), 2. Isoleucine, 3. Leucine, 4. Valine, 5. Ethanol, 6. -(CH_2)n-, 7.Lactate, 8. Threonine, 9. Alanine, 10. Acetate, 11. N-acetylglucosamine, 12. Glutamate, 13. Acetoacetate, 14. Pyruvate, 15. Glutamine, 16. Citrate, 17. –CH═CH–CH_2–CH═CH-, 18. Lysine, 19. Creatine, 20. Choline, 21. Acetylcholine, 22. Glucose-6-phosphate, 23. Proline, 24. Methanol 25. Myo-inositol, 26. Glucose, 27. Glycerol, 28. Creatinine, 29. Triacylglycerol (–CH_2–OCO-), 30. –CH═CH-, 31. Glucose-1-phosphate, 32. Uracil, 33. Tyrosine, 34. Phenylalanine, 35. Histamine, 36. Hypoxanthine, 37. Inosine.

(PLS-DA) was used to generate a predictive model with the obtained variables. CV (Venetian blinds) was used to select the finest number of latent variables for the model. The model was refined and OPLS-DA model was calculated. In order to determine the goodness of the model to discriminate between different sets of samples, a receiver operating characteristic (ROC) was generated, and the area under the curve (AUC), sensitivity and specificity were calculated. The robustness and over-fitting of the model were tested through permutation tests (100 iterations).

2.6. Univariate statistical analysis

Univariate statistical analysis was performed on the data from atheroma plaque and serum. The Shapiro-Wilks test was applied to check the normality of the variables included in the study. Subsequently, *t*-test or U de Mann Whitney test were used, when appropriate, for the comparison of the means of the relative concentrations of the analysed metabolites. Based on previous publications, an FDR threshold <0.2 was established [25–30].

In addition, the relationship between metabolic changes in atheroma plaques and sera was explored in the 35 paired plaque and serum samples. For this purpose, the Pearson correlation coefficient and the bilateral significance of the correlation between the two sets of variables (atheroma plaque data versus serum data) were calculated.

IBM SPSS Statistics 25 version was used for univariate statistics.

2.7. Metabolite set enrichment analysis

To investigate which metabolic pathways could be involved in plaque vulnerability, *Metaboanalyst* [31] was used. HMDB ID of each metabolite was used to include them in the enrichment analysis. The lipid motifs and unknown metabolites were excluded from the analysis. The metabolite set library chosen for the analysis was the one based on the KEGG human metabolic pathways. Pathways with a p-value <0.1 and impact >0 were considered to be significant.

3. Results and discussion

Plaques from symptomatic and asymptomatic patients, as previously defined, have been analysed by NMR spectroscopy to identify differences in the metabolome that might be associated with plaque vulnerability. Serum samples obtained from patients with and without clinical symptomatology were also analysed. A total of 70 serum samples and 38 atheroma plaque samples were included, 35 of which were paired plaque and serum samples from the same patient. Both groups were balanced in terms of age, sex, and main cardiovascular risk factors. (Table 1). PCA analyses revealed no clustering of patients by sex or symptomatology in either the atheroma plaque or serum samples (Figs. S1 and S2).

Table 2
Annotation of the metabolites present in serum and plaque samples. The sample type, the group responsible for the NMR signal, chemical shift, multiplicity, and J coupling are displayed. To simplify, only one signal per metabolite is shown in the table.

Number assignment	Metabolite	Sample type	Group	Chemical Shift (ppm)	Multiplicity and J coupling (Hz)[a]
1	Fatty Acids (–CH_2–CH_3)	Plaque/Serum	CH_3	0.83	–
2	Isoleucine	Serum	σCH_3	0.93	t, J = 7.41
3	Leucine	Serum	σCH_3	0.95	t, J = 5.89
4	Valine	Plaque/Serum	γXH_3	0.98	d, J = 7.2
5	Ethanol	Plaque/Serum	CH_2	1.16	t, J = 7.08
6	-$(CH_2)_n$-	Plaque/Serum	CH_2	1.26	–
7	Lactate	Plaque/Serum	CH_3	1.32	d, J = 7.00
8	Threonine	Serum	γXH_3	1.33	d, J = 6.58
9	Alanine	Plaque/Serum	βXH_3	1.48	d, J = 7.40
10	Acetate	Serum	CH_3	1.91	s
11	N-acetylglucosamine	Plaque/Serum	CH_3	2.03	s
12	Glutamate	Plaque	βXH_2	2.13	m
13	Acetoacetate	Serum	CH_3	2.27	s
14	Pyruvate	Plaque/Serum	CH_3	2.36	s
15	Glutamine	Serum	γCH_2	2.46	m, J = 14.4, 6.8
16	Citrate	Plaque/Serum	CH_2	2.52	d, J = 15.80
17	-CH═CH–CH_2–CH═CH-	Plaque/Serum	CH_2	2.79	–
18	Lysine	Plaque/Serum	CH_2	3.09	t, J = 6.50
19	Creatine	Plaque/Serum	CH_3	3.02	s
20	Choline	Plaque/Serum	-N^+-$(CH_3)_3$	3.19	s
21	Acetylcholine	Plaque/Serum	-N^+-$(CH_3)_3$	3.21	s
22	Glucose-6-phosphate	Plaque	CH_2	3.25	dd, J = 9.21, 7.99
23	Proline	Plaque/Serum	CH_2	3.33	m
24	Methanol	Plaque/Serum	CH_3	3.35	s
25	Myo-inositol	Plaque	C1HC3H	3.59	dd, J = 3.4, 2.5
26	Glucose	Plaque/Serum	C6H u	3.60	m
27	Glycerol	Serum	1,3 CH_2OH	3.65	m
28	Creatinine	Serum	CH_2	4.09	s
29	Tryacilglicerols	Plaque	-CH_2-OCO-	4.30	–
30	-CH═CH-	Plaque/Serum	CH	5.28	–
31	Glucose-1-phosphate	Plaque	C1H	5.42	s
32	Uracil	Plaque	C6H	5.84	–
33	Tyrosine	Serum	CH 2,6	7.19	m
34	Phenylalanine	Serum	CH 2,6	7.27	m
35	Histamine	Serum	CH	7.79	s
36	Hypoxanthine	Plaque	CH	8.17	s
37	Inosine	Plaque	CH	8.22	s

[a] The multiplicity of the signals is indicated as s: singlet; d: doublet, t: triplet, m: multiplet, dd: doublet of doublets.

3.1. Metabolic profiling of atherosclerotic plaque tissues and serum samples

The signals in the spectra were assigned to the corresponding metabolites for atheroma plaques and serum samples (Fig. 1). In the tissue spectra, due to the importance of the broad and intense signals coming from molecules such as lipids or lipoproteins, the identification of smaller signals produced by metabolites was challenging. Nevertheless, we were able to identify a total of 26 metabolites; 6 of them were amino acids, and 5 were fatty acids, among others (Table 2). In serum samples, a total of 29 metabolites were identified (Table 2), 10 of them were amino acids, and 6 were fatty acids. Remarkably, 18 of the 37 metabolites identified were found both in tissue and serum samples. To explore whether the serum metabolic pattern could reflect local dysregulation, a correlation analysis was performed for these 18 metabolites in the subset of 35 paired tissue and serum samples. Among all the analysed metabolites, valine exhibited a positive correlation in both sample types ($r = 0.375$, $p < 0.05$), becoming a potential circulating biomarker of that occurring at the plaque local site (Supplementary Table S1).

3.2. Identification of potential biomarkers of vulnerability in plaque and serum

PLS-DA was performed in both serum and tissue data. Cross-validated models were generated to discriminate between plaques from symptomatic and asymptomatic patients.

For the atheromatous plaque tissue analysis, a total of 120 signals (variables) were integrated from the NMR spectra. GA was applied to the data matrix, and the best model was obtained with a total of 23 variables. The resultant PLS-DA, using 3 principal components, was able to correctly classify stable and vulnerable plaques with 100 % sensitivity and 91.6 % specificity (Fig. S3). The model was orthogonalized and OPLS-DA model was calculated. The ROC curve rendered an AUC value of 0.985, showing the excellent classification capacity of the model (Fig. 2). The model was statistically significant ($p < 0.05$) for all the permutation tests. The metabolites included in the model were threonine, alanine, glutamate, citrate, myo-inositol, glucose, creatine, lactate, uracil, hypoxanthine, inosine, lipid fragments –$(CH_2)_n$-, –CH═CH- and –CH═CH–CH_2–CH═CH-, and two unknown compounds (Table 3). All the metabolites in vulnerable plaques were increased. Moreover, myo-inositol and glutamate showed significant differences between plaques from symptomatic and asymptomatic patients ($p = 0.011$ and 0.006 respectively), and the –CH═CH- lipid motif was close to significance ($p = 0.055$) according to the univariate analysis (Table 3). Furthermore, fold change values and individual AUC values for each metabolite are displayed in Table 3. Also, sensitivity and specificity of the most relevant metabolites are summarized in the Supplementary Table S2.

Our findings regarding myo-inositol levels in atherosclerotic plaques presented an unexpected result. While previous research has associated decreased circulating myo-inositol with various pathological conditions [32], the local dysregulation of myo-inositol within atherosclerotic plaques has been scarcely investigated. In our study, we observed elevated myo-inositol levels associated with symptomatic plaques. Interestingly, a recent study by Jin et al. [33] reported decreased

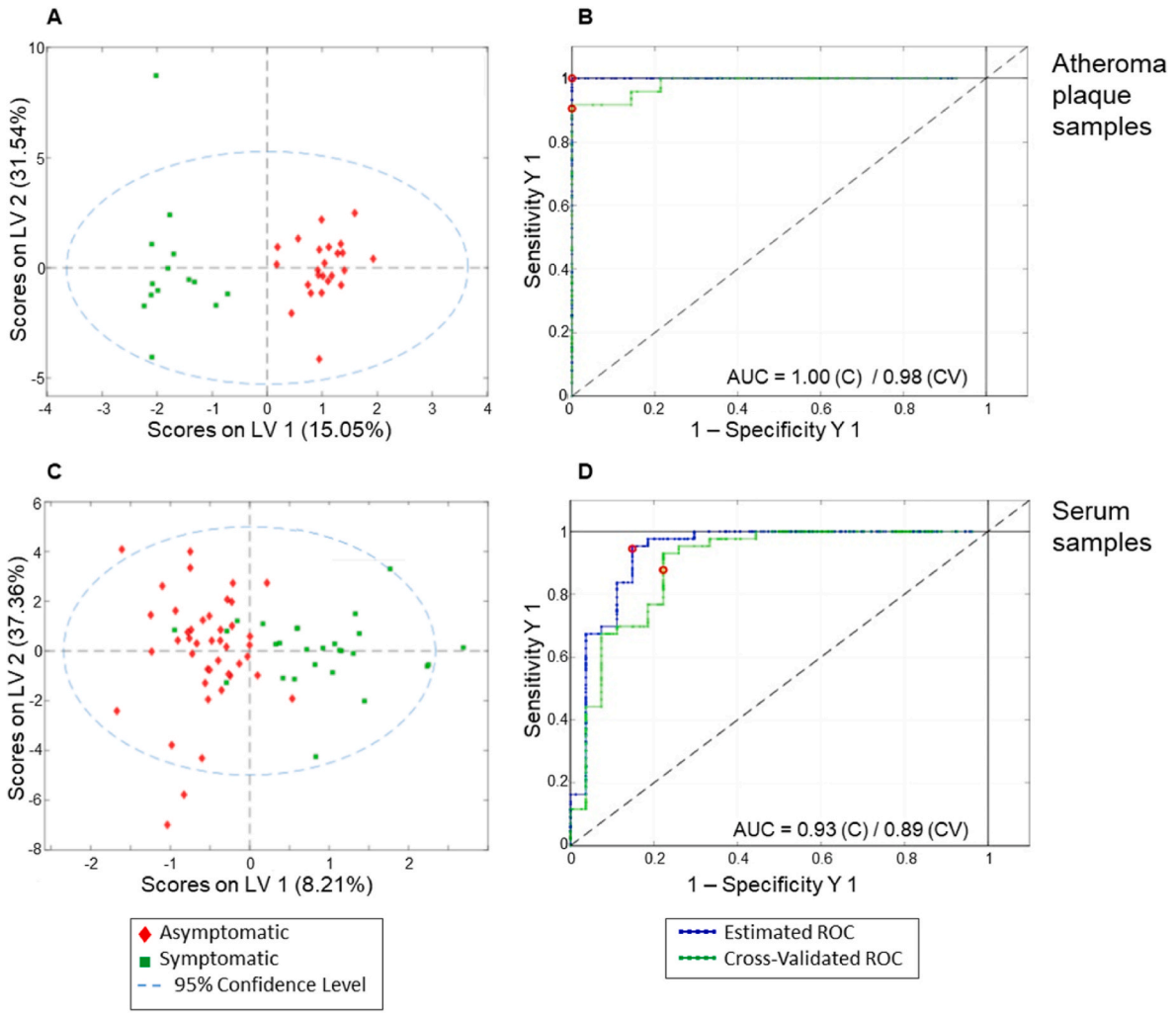

Fig. 2. OPLS-DA model graphs and ROC curve with AUC values obtained based on the variables selected by the application of genetic algorithms. A) OPLS-DA samples classification of the plaque samples. B) ROC curve for the discriminative model of plaque samples. Calibration and CV results are shown. An AUC value of 0.98 for the CV is reached. C) OPLS-DA samples classification of the serum samples. D) ROC curve of the classification of the estimated (blue) and calibrated (green) of the serum samples. An AUC value of 0.89 is obtained. Asymptomatic samples are represented by red diamonds and symptomatic samples by green squares.

myo-inositol levels specifically associated with intraplaque hemorrhage and, consequently, plaque instability. It is noteworthy that Jin et al. only included symptomatic patients, leaving the myo-inositol levels in asymptomatic patients unexplored. Nevertheless, it is worth noting that, although myo-inositol showed significant differences between plaque samples ($p = 0.011$) and a fold change >1.5, FDR was >0.2 thus indicating that these differences could be stochastical. Further studies will help to elucidate the potential role of local myo-inositol concentration in plaque instability.

Regarding to glutamate, previous studies have shown that an increase in plasma levels is related to a higher risk of cardiovascular diseases (CVD). Plasma glutamate levels were associated with an increased risk of stroke in a study performed in 980 participants under follow up, and found that baseline glutamate was associated with 43 % and 81 % increased risk of CVD and stroke, respectively [34]. These results were validated by a different study where type 2 diabetes mellitus patients showed a positive correlation between glutamate plasma levels and the risk of stroke [35]. Moreover, Gallina et al. reported that VSMCs within human atherosclerotic plaques expressed AMPA-type glutamate receptors. Notably, the expression of these receptors was lower in plaques from symptomatic patients compared to asymptomatic individuals. The authors hypothesized that these receptors might play a role in VSMC phenotypic switching [36]. In conjunction with our findings, it appears plausible that a decrease in VSMC AMPA-type glutamate receptors in vulnerable plaques could lead to intracellular glutamate accumulation.

In the analysis of serum samples, a total of 130 signals from the spectra were integrated. Representative signals from each metabolite were included as variables for the PLS-DA model, with a total of 32 variables. After applying GA, 12 variables were selected for the discriminative model. The final model was able to classify the serum of asymptomatic from symptomatic patients with an 88.37 % sensitivity and a 77.78 % specificity. The AUC value was 0.89 (Fig. 2b). The discriminant metabolites were threonine, histamine, acetoacetate, methanol, isoleucine, valine, lysine, alanine, lactate, and the lipid motifs $–CH_2–CH_3–$ and –CH═CH-. The model was also significant for all the permutation tests. Moreover, according to the univariate analysis, threonine and –CH═CH- showed a significant difference ($p = 0.000$ and 0.015 respectively), and histamine was close to significance ($p = 0.055$), with an increase in the serum of symptomatic patients for the three metabolites (Table 3). For the serum samples, the fold change and AUC values for each metabolite are also displayed in Table 3.

As it has been observed in this study, an increase in the concentration of histamine has previously been related to the occurrence of cardiovascular events [37]. Blood histamine levels are increased in the inflammatory process produced in unstable plaques [38]. Histamine is an inflammatory mediator produced from L-histidine released from mast

Table 3
Metabolites participating in the discriminative models of asymptomatic *vs.* symptomatic plaques and sera.

	Metabolites	VIPs[a] PLS-DA	VIPs[a] OPLS-DA	AUC	p-value	FDR	Fold Change	Trend[b]
Plaque	***Myo-inositol***	1.989	1.341	0.720	**0.011**	0.258	1.871	↑
	Glutamate	1.768	1.769	0.771	**0.006**	0.152	1.948	↑
	-CH═CH-	1.511	1.594	0.744	0.055	0.259	1.668	↑
	Glucose	1.063	0.864	0.696	0.224	0.387	1.414	↑
	Threonine	0.988	0.407	0.639	0.341	0.435	1.246	↑
	Hypoxanthine	0.947	0.563	0.533	0.715	0.747	1.292	↑
	$-(CH_2)_n-$	0.861	0.756	0.619	0.286	0.546	1.332	↑
	$-CH═CH–CH_2–CH═CH-$	0.828	1.239	0.687	0.068	0.258	1.553	↑
	Lactate	0.747	0.659	0.598	0.274	0.387	1.216	↑
	Uracil	0.737	0.619	0.550	0.304	0.467	1.338	↑
	Citrate	0.675	1.139	0.655	0.171	0.346	1.685	↑
	2-aminobutyrate	0.558	0.881	0.622	0.107	0.346	1.331	↑
	Glucose-1-phosphate	0.533	0.902	0.639	0.135	0.283	1.366	↑
	Inosine	0.526	0.902	0.545	0.421	0.484	1.583	↑
	Creatine	0.517	0.942	0.639	0.201	0.348	1.439	↑
Serum	***Threonine***	1.887	2.200	0.750	**0.000**	0.011	1.356	↑
	-CH═CH-	1.431	1.826	0.672	**0.015**	0.167	1.295	↑
	Histamine	1.179	1.167	0.637	0.056	0.257	1.108	↑
	Acetoacetate	0.973	0.052	0.537	0.606	0.758	0.995	↓
	$-CH_2-CH_3$	0.868	0.657	0.599	0.277	0.759	0.927	↓
	Methanol	0.829	0.852	0.544	0.540	0.721	0.804	↓
	Isoleucine	0.701	0.777	0.605	0.198	0.406	0.802	↓
	Valine	0.700	0.257	0.586	0.672	0.440	1.031	↑
	Lysine	0.642	0.145	0.512	0.876	0.935	1.010	↓
	Alanine	0.511	0.544	0.581	0.258	0.444	1.047	↑
	Lactate	0.493	0.335	0.535	0.613	0.759	0.962	↓

[a] VIP: Variable importance in projection, represents the importance of the metabolite in the discriminative capacity of the model.
[b] The arrow direction indicates the change in concentration of symptomatic compared to asymptomatic patients. Metabolites with significant differences ($p < 0.05$) are shown in bold.

cells. The accumulation of activated mast cells and histamine in the atherosclerotic lesion has been associated with the vulnerability of the plaque [39]. Blood vessels dilatation, increased vascular permeability, and the migration of leukocytes into the atheroma plaque are among the effects of high levels of histamine in blood. Furthermore, histamine can trigger the production of the glycoprotein tissue factor (TF) by endothelial cells and smooth muscle cells [40]. TF, usually encrypted in the endothelial cells, is a key protein that triggers coagulation through the extrinsic pathway once exposed to the blood flow, leading to thrombin formation [41], and contributes to the development of thrombosis within the atherosclerotic arteries [40].

We have also found elevated levels of threonine in serum samples from patients with symptomatic carotid stenosis. This finding contrasts with previous research where higher circulating levels of threonine were inversely related to peripheral artery disease PAD [42] or heart failure [43]. However, considering threonine's role in the tricarboxylic acid cycle, providing ATP and α-ketoglutarate for brain metabolism [44,45], its elevation in our patients might be attributed to an adaptive response to ischemic brain injury. In fact Wang et al. showed increased threonine levels in patients with favorable stroke outcomes [46]. Since our samples were collected days post-ischemic event, it is plausible that elevated threonine levels are a consequence of the event, serving as a mechanism for repairing brain injury.

It is worth noting that some of the circulating metabolites included in

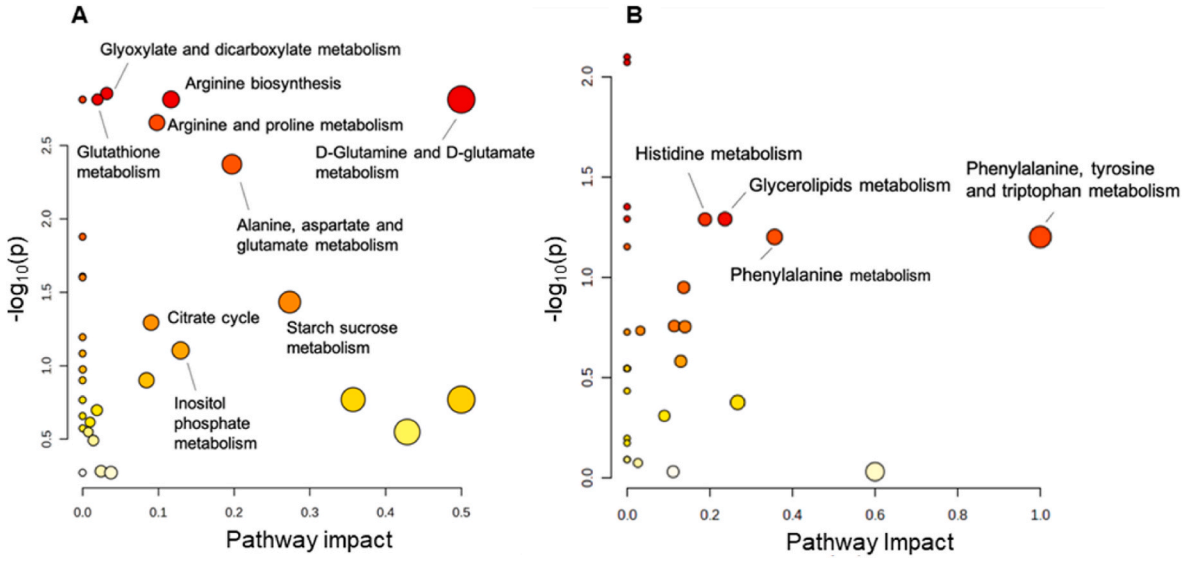

Fig. 3. A) Metabolic pathways related to plaque vulnerability based on the metabolites found in the plaque. B) Metabolic pathways related to plaque vulnerability based on the metabolites found in the serum.

Table 4
Metabolic pathways involved in plaque vulnerability, based on the differences in the metabolites found in the plaques.

Metabolic pathway	Metabolites	p-value	Impact[a]
Glyoxylate and dicarboxylate metabolism	L-Glutamate, Citrate	0.0014	0.03
D-Glutamine and D-glutamate metabolism	L-Glutamate	0.0015	0.50
Arginine biosynthesis	L-Glutamate	0.0015	0.12
Glutathione metabolism	L-Glutamate	0.0015	0.02
Arginine and proline metabolism	Creatine, L-Glutamate	0.002	0.10
Alanine, aspartate and glutamate metabolism	L-Alanine, L-Glutamate, Citrate	0.004	0.20
Starch and sucrose metabolism	Glucose-1-P, Glucose-6-P	0.036	0.27
Citrate cycle (TCA[b] cycle)	Citrate	0.05	0.09
Inositol phosphate metabolism	Glucose-6-P, Myo-inositol	0.078	0.13

[a] Impact: Pathway impact value calculated from pathway topology analysis.
[b] Tricarboxylic Acid Cycle.

our model for discriminating symptomatic and asymptomatic patients have been previously related with cardiovascular events. A meta-analysis conducted by Wang et al. established a correlation between elevated isoleucine levels and an increased risk of cardiovascular diseases [47]. Additionally, inosine and hypoxanthine have been proposed as markers of cardiac ischemia [48], but their role in neurological ischemic events needs to be further studied.

3.3. Metabolic pathways involved in plaque vulnerability

Metaboanalyst 4.0 was used to generate a metabolite set enrichment analysis for the identification of biological patterns associated with the metabolomic data obtained from the serum and plaque samples. First, the metabolites are individually analysed to determine if they are significant, and later, the existence of meaningful patterns is determined. It can detect subtle but consistent differences among related compounds that conventional methods may not detect. We defined as notable differences those with a p-value <0.1 and an impact >0.

In atheroma plaque samples, nine metabolic pathways were potentially altered between symptomatic and asymptomatic patients. Six pathways were statistically significant with a p-value <0.05: glyoxylate and dicarboxylate metabolism, D-glutamine and D-glutamate metabolism, arginine biosynthesis, arginine, and proline metabolism, alanine, aspartate and glutamate metabolism, starch and sucrose metabolism, and three pathways notably altered (p-value <0.1): citrate cycle (TCA cycle), valine, leucine and isoleucine biosynthesis, and inositol phosphate metabolism (Fig. 3A).

Our results are consistent with the fact that both groups are composed of individuals with atherosclerosis, which may lead to discrete changes in the metabolic profiles. The p-value was set to 0.1 due to the limited number of samples but also because subtle differences were expected to be observed as it is not anticipated that the metabolism of cells in vulnerable and stable plaques will produce substantial changes, and even smaller changes are expected to be reflected in the bloodstream.

As detailed in Table 4, glutamate is a common metabolite in the pathways. As it has been previously referred, increased glutamate levels are positively correlated with cardiovascular risk. Also, circulating glutamate has been associated with subclinical atherosclerosis independently of other risk factors [49]. In fact, glutamate-mediated excitotoxicity has been previously proposed as a potential therapeutic target for ischemic stroke [50]. Besides, citrate and citric acid metabolism has also previously been related to increased risk in different CVD [51,52].

In serum samples, there were four pathways notably altered between symptomatic and asymptomatic patients: histidine metabolism, glycerolipids metabolism, phenylalanine metabolism, and phenylalanine, tyrosine, and tryptophan metabolism (Fig. 3B). The alteration in the metabolism of amino acids has previously been reported to be involved in the development of atherosclerosis [53]. More specifically, the levels of phenylalanine and tyrosine have been associated with an increased risk of coronary artery disease and stroke [54]. Accordingly, differences in metabolic pathways where phenylalanine and tyrosine are participating occur between symptomatic and asymptomatic patients (Table 5). The relevance of histamine and histidine metabolism has already been discussed.

Table 5
Metabolic pathways involved in plaque vulnerability, based on the differences in the metabolites found in serum.

Metabolic pathway	Metabolites	p-value	[a]Impact
Glycerolipid metabolism	Glycerol	0.051	0.24
Histidine metabolism	Histamine	0.052	0.19
Phenylalanine, tyrosine, and tryptophan biosynthesis	Phenylalanine, Tyrosine	0.063	1.0
Phenylalanine metabolism	Phenylalanine, Tyrosine	0.063	0.036

[a] Impact: Pathway impact value calculated from pathway topology analysis.

4. Conclusions

We have performed a preliminary study in plaques and serum samples from patients with carotid stenosis by NMR. We have sought biomarkers of plaque vulnerability through the generation of statistical models able to discriminate symptomatic and asymptomatic patients with high sensitivity (100 % and 88.37 %) and specificity (91.6 % and 77.78 %) in plaque and serum, respectively. Increased concentration of myo-inositol, glutamate, and fatty acids was found in vulnerable plaques, whereas an increase in histamine, threonine, and fatty acids was observed in serum samples. Overall, the data presented herein provided valuable information on potential biomarkers of plaque vulnerability, both in plaque and serum samples. Although the presence of biomarkers in plaque is not of high value from a diagnosis perspective (as it implies the extraction of the plaque), the molecular mechanism involved in plaque vulnerability is still unknown, and the metabolites and metabolic pathways described in this work could be a starting point to understand better the reasons why some plaques become vulnerable and other remain stable. Also, locally dysregulated metabolites could highlight new therapeutic targets. On the other hand, the analysis of metabolites present in serum of symptomatic and asymptomatic patients could be studied as biomarkers of risk of plaque rupture. As previously mentioned, histamine, phenylalanine, and tyrosine, which are described in this work as potential biomarkers of plaque rupture, have already been associated with plaque vulnerability.

A limitation of this study is the sample size. However, it is noteworthy that obtaining carotid plaque specimens from both symptomatic and asymptomatic patients is exceptionally valuable. In fact, our sample size ($n = 38$ distinct carotid plaques) is comparable to or even exceeds those of similar studies employing different metabolomics techniques [55–59]. Only the study by Tomas et al. [20] included a larger number of patients, although their analysis was restricted to a targeted metabolomics assessment of a limited set of metabolites, which limits the ability to discover novel metabolites involved. Our positive results endorse the performance of validation studies in an independent external cohort of patients to establish the role of these metabolites as biomarkers of plaque vulnerability.

Moreover, given the exploratory nature of our study, we adopted an FDR threshold of 0.2, consistent with previous prospective metabolomics analyses [25–30]. As a result, our findings were marginally significant and may contain a degree of stochastic variability. Consequently, further studies with a larger number of participants would be

necessary to validate our results. Finally, our samples were obtained when the ischemic event had already occurred; thus, causality cannot be established with complete confidence. A longitudinal and a follow-up study should be performed to understand the applicability of our results better.

CRediT authorship contribution statement

Marina Botello-Marabotto: Writing – original draft, Visualization, Investigation, Formal analysis, Data curation. **Emma Plana:** Writing – review & editing, Project administration, Methodology, Investigation, Funding acquisition. **M. Carmen Martínez-Bisbal:** Writing – review & editing, Project administration, Methodology, Investigation. **Pilar Medina:** Writing – review & editing, Investigation. **Andrea Bernardos:** Writing – review & editing, Investigation. **Ramón Martínez-Máñez:** Writing – review & editing, Supervision, Resources, Funding acquisition, Conceptualization. **Manuel Miralles:** Writing – review & editing, Supervision, Resources, Funding acquisition, Conceptualization.

Declaration of competing interest

The authors declare that they have no known competing financial interests or personal relationships that could have appeared to influence the work reported in this paper.

Acknowledgments

M. Botello-Marabotto acknowledges Generalitat Valenciana and the Spanish Government for her PhD grants ACIF/2020 and FPU 2020, respectively. Andrea Bernardos acknowledges her "Beatriz Galindo" contract from the MCIN (BG20/00020). This project has received the following funding: *Instituto de Salud Carlos III (*ISCIII*) (PI20/01171 and PI20/00075) co*-funded *by the European Union* (ERDF, "A way to make Europe"), project PID2021-126304OB-C41 and PID2021-128141OB-C22 funded by MCIN/AEI/10.13039/501100011033/and by European Regional Development Fund - A way of doing Europe and Generalitat Valenciana (project CIPROM/2021/007). La Fe Biobank (Hospital Universitario y Politécnico La Fe) is acknowledged for the storage and management of tissue samples (PT17/0015/0043). CIBER -Consorcio Centro de Investigación Biomédica en Red- (CB07/01/2012), Ministerio de Ciencia e Innovación and U26 NMR: Biomedical Applications II platform from Nanbiosis (Research Infrastructures & Services of CIBER-BBN) are also gratefully acknowledged.

Appendix A. Supplementary data

Supplementary data to this article can be found online at https://doi.org/10.1016/j.talanta.2024.127211.

Glossary of field-specific terms

AUC	Area Under the Curve
BMI	Body Mass Index
COPD	Chronic Obstructive Pulmonary Disease
CRF	Chronic Renal Failure
CV	Cross-Validation
CVD	Cardiovascular Diseases
DSS-d_6	Deuterated 3-(trimethylsilyl)-1-propanesulfonic acid sodium salt
GA	Genetic Algorithms
HMDB	Human Metabolome Database
HRMAS	High-Resolution Magic Angle Spinning
KEGG	Kyoto Encyclopedia of Genes and Genomes
LDL	Low Density Lipoproteins
MS	Mass Spectrometry
NMR	Nuclear Magnetic Resonance
OPLS-DA	Orthogonal Partial Least Squares-Discriminant Analysis
ox-LDL	Oxidized Low Density Lipoproteins
PAD	Peripheral Artery Disease
PLS-DA	Partial Least Squares-Discriminant Analysis
ROC	Receiver Operating Characteristic
TF	Tissue Factor
UHPLC–MS	Ultra-High Performance Liquid Chromatography Mass Spectrometry
VSMC	Vascular Smooth Muscle Cells

Data availability

Data will be made available on request.

References

[1] C. Mattiuzzi, G. Lippi, Worldwide disease epidemiology in the older persons, Eur. Geriatr. Med. 11 (2020) 147–153, https://doi.org/10.1007/s41999-019-00265-2.
[2] C. Banerjee, M.I. Chimowitz, Stroke caused by atherosclerosis of the Major intracranial arteries, Circ. Res. 120 (2017) 502–513, https://doi.org/10.1161/CIRCRESAHA.116.308441.
[3] G.K. Hansson, Inflammation, atherosclerosis, and coronary artery disease, N. Engl. J. Med. 325 (2005) 1685–1695, https://doi.org/10.1056/NEJMra043430.
[4] G.K. Hansson, A. Hermansson, The immune system in atherosclerosis, Nat. Immunol. 12 (2011) 204–212, https://doi.org/10.1038/ni.2001.
[5] R. Virmani, A.P. Burke, A. Farb, F.D. Kolodgie, Pathology of the unstable plaque, Prog. Cardiovasc. Dis. 44 (2002) 349–356, https://doi.org/10.1053/pcad.2002.122475.
[6] G.A.N. Gowda, S. Zhang, H. Gu, V. Asiago, N. Shanaiah, D. Raftery, Metabolomics-based methods for early disease diagnostics, Expert Rev. Mol. Diagn. 8 (2008) 617–633, https://doi.org/10.1586/14737159.8.5.617.
[7] V. Tounta, Y. Liu, A. Cheyne, G. Larrouy-Maumus, Metabolomics in infectious diseases and drug discovery, Mol. Omi. 17 (2021) 376–393, https://doi.org/10.1039/d1mo00017a.
[8] M. Botello-Marabotto, M.C. Martínez-Bisbal, M. Calero, A. Bernardos, A.B. Pastor, M. Medina, R. Martínez-Máñez, Non-invasive biomarkers for mild cognitive impairment and Alzheimer's disease, Neurobiol. Dis. 187 (2023), https://doi.org/10.1016/j.nbd.2023.106312.
[9] A. Loras, C. Suárez-Cabrera, M.C. Martínez-Bisbal, G. Quintás, J.M. Paramio, R. Martínez-Máñez, S. Gil, J.L. Ruiz-Cerdá, Integrative metabolomic and transcriptomic analysis for the study of bladder cancer, Cancers 11 (2019), https://doi.org/10.3390/cancers11050686.

[10] A. Loras, M.C. Martínez-Bisbal, G. Quintás, S. Gil, R. Martínez-Máñez, J.L. Ruiz-Cerdá, Urinary metabolic signatures detect recurrences in non-muscle invasive bladder cancer, Cancers 11 (2019) 914, https://doi.org/10.3390/cancers11070914.
[11] J. Oto, Á. Fernández-Pardo, M. Roca, E. Plana, F. Cana, R. Herranz, J. Pérez-Ardavín, C.D. Vera-Donoso, M. Martínez-Sarmiento, P. Medina, LC–MS metabolomics of urine reveals distinct profiles for non-muscle-invasive and muscle-invasive bladder cancer, World J. Urol. 40 (2022) 2387–2398, https://doi.org/10.1007/s00345-022-04136-7.
[12] J. Oto, Á. Fernández-Pardo, M. Roca, E. Plana, M.J. Solmoirago, J.V. Sánchez-González, C.D. Vera-Donoso, M. Martínez-Sarmiento, F. España, S. Navarro, P. Medina, Urine metabolomic analysis in clear cell and papillary renal cell carcinoma: a pilot study, J. Proteonomics 218 (2020) 103723, https://doi.org/10.1016/j.jprot.2020.103723.
[13] A. D'Alessandro, B. Giardina, G. Federica, A.M. Timperio, L. Zolla, Clinical metabolomics: the next stage of clinical biochemistry, Blood Transfus 10 (2012) 19–24, https://doi.org/10.2450/2012.005S.
[14] J.L. Ward, J.M. Baker, S.J. Miller, C. Deborde, M. Maucourt, B. Biais, D. Rolin, A. Moing, S. Moco, J. Vervoort, A. Lommen, H. Schäfer, E. Humpfer, M.H. Beale, An inter-laboratory comparison demonstrates that [1H]-NMR metabolite fingerprinting is a robust technique for collaborative plant metabolomic data collection, Metabolomics 6 (2010) 263–273, https://doi.org/10.1007/s11306-010-0200-4.
[15] M.C. Martínez-Bisbal, L. Martí-Bonmatí, J. Piquer, A. Revert, P. Ferrer, J.L. Llácer, M. Piotto, O. Assemat, B. Celda, 1H and 13C HR-MAS spectroscopy of intact biopsy samples ex vivo and in vivo 1H MRS study of human high grade gliomas, NMR Biomed. 17 (2004) 191–205, https://doi.org/10.1002/nbm.888.
[16] B. Martínez-Granados, D. Monleón, M.C. Martínez-Bisbal, J.M. Rodrigo, J. del Olmo, P. Lluch, A. Ferrández, L. Martí-Bonmatí, B. Celda, Metabolite identification in human liver needle biopsies by high-resolution magic angle spinning 1H NMR spectroscopy, NMR Biomed. 19 (2006) 90–100, https://doi.org/10.1002/nbm.1005.
[17] M.C. Martínez-Bisbal, D. Monleon, O. Assemat, M. Piotto, J. Piquer, J.L. Llácer, B. Celda, Determination of metabolite concentrations in human brain tumour biopsy samples using HR-MAS and ERETIC measurements, NMR Biomed. 22 (2009) 199–206, https://doi.org/10.1002/nbm.1304.
[18] P. Würtz, J.R. Raiko, C.G. Magnussen, P. Soininen, A.J. Kangas, T. Tynkkynen, R. Thomson, R. Laatikainen, M.J. Savolainen, J. Laurikka, P. Kuukasjärvi, M. Tarkka, P.J. Karhunen, A. Jula, J.S. Viikari, M. Kähönen, T. Lehtimäki, M. Juonala, M. Ala-Korpela, O.T. Raitakari, High-throughput quantification of circulating metabolites improves prediction of subclinical atherosclerosis, Eur. Heart J. 33 (2012) 2307–2316, https://doi.org/10.1093/eurheartj/ehs020.
[19] P.A. Vorkas, J. Shalhoub, G. Isaac, E.J. Want, J.K. Nicholson, E. Holmes, A. H. Davies, Metabolic phenotyping of atherosclerotic plaques reveals latent associations between free cholesterol and ceramide metabolism in atherogenesis, J. Proteome Res. 14 (2015) 1389–1399, https://doi.org/10.1021/pr5009898.
[20] L. Tomas, A. Edsfeldt, I.G. Mollet, L.P. Matic, C. Prehn, J. Adamski, G. Paulsson-Berne, U. Hedin, J. Nilsson, E. Bengtsson, I. Gonçalves, H. Björkbacka, Altered metabolism distinguishes high-risk from stable carotid atherosclerotic plaques, Eur. Heart J. 39 (2018) 2301–2310, https://doi.org/10.1093/eurheartj/ehy124.
[21] O. Beckonert, H.C. Keun, T.M.D. Ebbels, J. Bundy, E. Holmes, J.C. Lindon, J. K. Nicholson, Metabolic profiling, metabolomic and metabonomic procedures for NMR spectroscopy of urine, plasma, serum and tissue extracts, Nat. Protoc. 2 (2007) 2692–2703, https://doi.org/10.1038/nprot.2007.376.
[22] D.S. Wishart, D. Tzur, C. Knox, R. Eisner, A.C. Guo, N. Young, D. Cheng, K. Jewell, D. Arndt, S. Sawhney, C. Fung, L. Nikolai, M. Lewis, M.A. Coutouly, I. Forsythe, P. Tang, S. Shrivastava, K. Jeroncic, P. Stothard, G. Amegbey, D. Block, D.D. Hau, J. Wagner, J. Miniaci, M. Clements, M. Gebremedhin, N. Guo, Y. Zhang, G. E. Duggan, G.D. MacInnis, A.M. Weljie, R. Dowlatabadi, F. Bamforth, D. Clive, R. Greiner, L. Li, T. Marrie, B.D. Sykes, H.J. Vogel, L. Querengesser, HMDB: the human metabolome database, Nucleic Acids Res. 35 (2007) 521–526, https://doi.org/10.1093/nar/gkl923.
[23] Chenomx NMR Suite, Chenomx inc., (n.d.).
[24] R. Cavill, H.C. Keun, E. Holmes, J.C. Lindon, J.K. Nicholson, T.M.D. Ebbels, Genetic algorithms for simultaneous variable and sample selection in metabonomics, Bioinformatics 25 (2009) 112–118, https://doi.org/10.1093/bioinformatics/btn586.
[25] S.C. Moore, K.M. Mazzilli, J.N. Sampson, C.E. Matthews, B.D. Carter, M.C. Playdon, Y. Wang, V.L. Stevens, A metabolomics analysis of postmenopausal breast cancer risk in the cancer prevention study II, Metabolites 11 (2021) 95, https://doi.org/10.3390/metabo11020095.
[26] S.C. Moore, M.C. Playdon, J.N. Sampson, R.N. Hoover, B. Trabert, C.E. Matthews, R.G. Ziegler, A metabolomics analysis of body mass index and postmenopausal breast cancer risk, J. Natl. Cancer Inst. 110 (2018) 588–597, https://doi.org/10.1093/jnci/djx244.
[27] M.C. Playdon, R.G. Ziegler, J.N. Sampson, R. Stolzenberg-Solomon, H. J. Thompson, M.L. Irwin, S.T. Mayne, R.N. Hoover, S.C. Moore, Nutritional metabolomics and breast cancer risk in a prospective study, Am. J. Clin. Nutr. 106 (2017) 637–649, https://doi.org/10.3945/ajcn.116.150912.
[28] K.M. McClain, J.N. Sampson, J.L. Petrick, K.M. Mazzilli, R.E. Gerszten, C.B. Clish, M.P. Purdue, L. Lipworth, S.C. Moore, Metabolomic analysis of renal cell carcinoma in the prostate, lung, colorectal, and ovarian cancer screening trial, Metabolites 12 (2022) 1189, https://doi.org/10.3390/metabo12121189.
[29] M. Mehanna, C.W. McDonough, S.M. Smith, Y. Gong, J.G. Gums, A.B. Chapman, J. A. Johnson, R.M. Cooper-DeHoff, Influence of genetic west african ancestry on metabolomics among hypertensive patients, Metabolites 12 (2022) 783, https://doi.org/10.3390/metabo12090783.
[30] T.V. Nguyen, J.M. Reuter, N.W. Gaikwad, D.M. Rotroff, H.R. Kucera, A. Motsinger-Reif, C.P. Smith, L.K. Nieman, D.R. Rubinow, R. Kaddurah-Daouk, P.J. Schmidt, The steroid metabolome in women with premenstrual dysphoric disorder during GnRH agonist-induced ovarian suppression: effects of estradiol and progesterone addback, Transl. Psychiatry 7 (2017) e1193, https://doi.org/10.1038/tp.2017.146.
[31] J. Chong, O. Soufan, C. Li, I. Caraus, S. Li, G. Bourque, D.S. Wishart, J. Xia, MetaboAnalyst 4.0: towards more transparent and integrative metabolomics analysis, Nucleic Acids Res. 46 (2018) W486–W494, https://doi.org/10.1093/nar/gky310.
[32] E. Lepore, R. Lauretta, M. Bianchini, M. Mormando, C. Di Lorenzo, V. Unfer, Inositols depletion and resistance: principal mechanisms and therapeutic strategies, Int. J. Mol. Sci. 22 (2021) 6796, https://doi.org/10.3390/IJMS22136796, 22 (2021) 6796.
[33] H. Jin, C. Zhang, J. Nagenborg, P. Juhasz, A.V. Ruder, C.J.J.M. Sikkink, B.M. E. Mees, O. Waring, J.C. Sluimer, D. Neumann, P. Goossens, M.M.P.C. Donners, A. Mardinoglu, E.A.L. Biessen, Genome-scale metabolic network of human carotid plaque reveals the pivotal role of glutamine/glutamate metabolism in macrophage modulating plaque inflammation and vulnerability, Cardiovasc. Diabetol. 23 (2024) 240, https://doi.org/10.1186/s12933-024-02339-3.
[34] Y. Zheng, F.B. Hu, M. Ruiz-Canela, C.B. Clish, C. Dennis, J. Salas-Salvado, A. Hruby, L. Liang, E. Toledo, D. Corella, E. Ros, M. Fitó, E. Gómez-Gracia, F. Arós, M. Fiol, J. Lapetra, L. Serra-Majem, R. Estruch, M.A. Martínez-González, Metabolites of Glutamate Metabolism Are Associated With Incident Cardiovascular Events in the PREDIMED PREvención con DIeta MEDiterránea (PREDIMED) Trial, J. Am. Heart Assoc. 5 (2016), https://doi.org/10.1161/JAHA.116.003755.
[35] R.T. Li, Y. Li, B.W. Wang, X.Q. Gao, J.X. Zhang, F. Li, X.Y. Zhang, Z.Z. Fang, Relationship between plasma glutamate and cardiovascular disease risk in Chinese patients with type 2 diabetes mellitus by gender, Front. Endocrinol. 14 (2023) 1–7, https://doi.org/10.3389/fendo.2023.1095550.
[36] A.L. Gallina, U. Rykaczewska, R.C. Wirka, A.S. Caravaca, V.S. Shavva, M. Youness, G. Karadimou, M. Lengquist, A. Razuvaev, G. Paulsson-Berne, T. Quertermous, A. Gisterå, S.G. Malin, L. Tarnawski, L. Matic, P.S. Olofsson, AMPA-type glutamate receptors associated with vascular smooth muscle cell subpopulations in atherosclerosis and vascular injury, Front. Cardiovasc. Med. 8 (2021) 655869, https://doi.org/10.3389/FCVM.2021.655869/BIBTEX.
[37] M. Rosic, V. Zdravkovic, S. Pantovic, G. Rosic, A. Tomic-Lucic, N. Zdravkovic, M. Colic, Z. Obradovic, Histamine blood concentration in ischemic heart disease patients, J. Biomed. Biotechnol. 2011 (2011), https://doi.org/10.1155/2011/315709.
[38] S. Clejan, S. Japa, C. Clemetson, S.S. Hasabnis, O. David, J.V. Talano, Blood histamine is associated with coronary artery disease, cardiac events and severity of inflammation and atherosclerosis, J. Cell Mol. Med. 6 (2002) 583–592, https://doi.org/10.1111/j.1582-4934.2002.tb00456.x.
[39] S. Yamada, K.Y. Wang, A. Tanimoto, Y. Sasaguri, Novel function of histamine signaling in hyperlipidemia-induced atherosclerosis: histamine H1 receptors protect and H2 receptors accelerate atherosclerosis, Pathol. Int. 65 (2015) 67–80, https://doi.org/10.1111/pin.12246.
[40] K.A. Lindstedt, M.I. Mäyränpää, P.T. Kovanen, Mast cells in vulnerable atherosclerotic plaques - a view to a kill, J. Cell Mol. Med. 11 (2007) 739–758, https://doi.org/10.1111/j.1582-4934.2007.00052.x.
[41] J. Steffel, A. Akhmedov, H. Greutert, T.F. Lüscher, F.C. Tanner, Histamine induces tissue factor expression: implications for acute coronary syndromes, Circulation 112 (2005) 341–349, https://doi.org/10.1161/CIRCULATIONAHA.105.553735.
[42] C. Razquin, M. Ruiz-Canela, E. Toledo, C.B. Clish, M. Guasch-Ferré, J.F. García-Gavilán, C. Wittenbecher, A. Alonso-Gómez, M. Fitó, L. Liang, D. Corella, E. Gómez-Gracia, R. Estruch, M. Fiol, J.M. Santos-Lozano, L. Serra-Majem, E. Ros, F. Aros, J. Salas-Salvadó, F.B. Hu, M.A. Martínez-González, Circulating amino acids and risk of peripheral artery disease in the PREDIMED trial, Int. J. Mol. Sci. 24 (2023) 270, https://doi.org/10.3390/IJMS24010270/S1.
[43] Q.F. Zhou, F. Yang, Y. Dai, S. Chen, F.R. Zhang, L. Lu, Q.Y. Lu, Tyrosine to threonine ratio was related to heart failure with reduced or mildly reduced ejection fraction, ESC Hear, Fail. 11 (2024) 1567–1579, https://doi.org/10.1002/ehf2.14700.
[44] J. zhou Ye, X. min Lin, Z. xue Cheng, Y. bin Su, W. xin Li, F. man Ali, J. Zheng, B. Peng, Identification and efficacy of glycine, serine and threonine metabolism in potentiating kanamycin-mediated killing of Edwardsiella piscicida, J. Proteonomics 183 (2018) 34–44, https://doi.org/10.1016/j.jprot.2018.05.006.
[45] T.N. Kovalenko, G.A. Ushakova, I. Osadchenko, G.G. Skibo, S.G. Pierzynowski, Neuroprotective effects of 2-oxoglutarate in the experimental ischemia of hippocampus, J. Physiol. Pharmacol. 62 (2011) 239–246.
[46] X. Wang, T. Liu, H. Song, S. Cui, G. Liu, A. Christoforou, P. Flaherty, X. Luo, L. Wood, Q.M. Wang, Targeted metabolomic profiling reveals association between altered amino acids and poor functional recovery after stroke, Front. Neurol. 10 (2020) 1425, https://doi.org/10.3389/fneur.2019.01425.
[47] Y. Wang, K. Huang, F. Liu, X. Lu, J. Huang, D. Gu, Association of circulating branched-chain amino acids with risk of cardiovascular disease: a systematic review and meta-analysis, Atherosclerosis 350 (2022) 90–96, https://doi.org/10.1016/j.atherosclerosis.2022.04.026.
[48] D.E. Farthing, C.A. Farthing, L. Xi, Inosine and hypoxanthine as novel biomarkers for cardiac ischemia: from bench to point-of-care, Exp. Biol. Med. (Maywood). 240 (2015) 821–831, https://doi.org/10.1177/1535370215584931.
[49] A. Lehn-Stefan, A. Peter, J. MacHann, F. Schick, E. Randrianarisoa, M. Heni, R. Wagner, A.L. Birkenfeld, A. Fritsche, H.U. Häring, H. Staiger, N. Stefan, Elevated

circulating glutamate is associated with subclinical atherosclerosis independently of established risk markers: a cross-sectional study, J. Clin. Endocrinol. Metab. 106 (2021) E982–E989, https://doi.org/10.1210/clinem/dgaa898.

[50] Z. Shen, M. Xiang, C. Chen, F. Ding, Y. Wang, C. Shang, L. Xin, Y. Zhang, X. Cui, Glutamate excitotoxicity: potential therapeutic target for ischemic stroke, Biomed. Pharmacother. 151 (2022) 113125, https://doi.org/10.1016/j.biopha.2022.113125.

[51] J.L. Santos, M. Ruiz-Canela, C. Razquin, C.B. Clish, M. Guasch-Ferré, N. Babio, D. Corella, E. Gómez-Gracia, M. Fiol, R. Estruch, J. Lapetra, M. Fitó, F. Aros, L. Serra-Majem, L. Liang, M.Á. Martínez, E. Toledo, J. Salas-Salvadó, F.B. Hu, M. A. Martínez-González, Circulating citric acid cycle metabolites and risk of cardiovascular disease in the PREDIMED study, Nutr. Metab. Cardiovasc. Dis. 33 (2023) 835–843, https://doi.org/10.1016/j.numecd.2023.01.002.

[52] S. Stryeck, M. Gastrager, V. Degoricija, M. Trbušić, I. Potočnjak, B. Radulović, G. Pregartner, A. Berghold, T. Madl, S. Frank, Serum concentrations of citrate, tyrosine, 2- and 3- hydroxybutyrate are associated with increased 3-month mortality in acute heart failure patients, Sci. Rep. 9 (2019) 1–10, https://doi.org/10.1038/s41598-019-42937-w.

[53] K. Nitz, M. Lacy, D. Atzler, Amino acids and their metabolism in atherosclerosis, Arterioscler. Thromb. Vasc. Biol. 39 (2019) 319–330, https://doi.org/10.1161/ATVBAHA.118.311572.

[54] R. Jauhiainen, J. Vangipurapu, A. Laakso, T. Kuulasmaa, J. Kuusisto, M. Laakso, The association of 9 amino acids with cardiovascular events in Finnish men in a 12-year follow-up study, J. Clin. Endocrinol. Metab. 106 (2021) 3448–3454, https://doi.org/10.1210/clinem/dgab562.

[55] C. Stegemann, I. Drozdov, J. Shalhoub, J. Humphries, C. Ladroue, A. Didangelos, M. Baumert, M. Allen, A.H. Davies, C. Monaco, A. Smith, Q. Xu, M. Mayr, Comparative lipidomics profiling of human atherosclerotic plaques, Circ. Cardiovasc. Genet. 4 (2011) 232–242, https://doi.org/10.1161/CIRCGENETICS.110.959098.

[56] P.A. Vorkas, J. Shalhoub, M.R. Lewis, K. Spagou, E.J. Want, J.K. Nicholson, A. H. Davies, E. Holmes, Metabolic phenotypes of carotid atherosclerotic plaques relate to stroke risk: an exploratory study, Eur. J. Vasc. Endovasc. Surg. 52 (2016) 5–10, https://doi.org/10.1016/j.ejvs.2016.01.022.

[57] R. Ding, W. Guan, M. Yi, X. Qin, S. Wei, H. Lu, Y. Wang, C. Lin, F. Mei, H. Xu, L. Wu, Identification of metabolic components of carotid plaque in high-risk patients utilizing liquid chromatography-tandem mass spectrometry, Rapid Commun. Mass Spectrom. 38 (2024) e9763, https://doi.org/10.1002/rcm.9763.

[58] W. Li, J. Luo, F. Peng, R. Liu, X. Bai, T. Wang, X. Zhang, J. Zhu, X.Y. Li, Z. Wang, W. Liu, J. Wang, L. Zhang, X. Chen, T. Xue, C. Ding, C. Wang, L. Jiao, Spatial metabolomics identifies lipid profiles of human carotid atherosclerosis, Atherosclerosis 364 (2023) 20–28, https://doi.org/10.1016/j.atherosclerosis.2022.11.019.

[59] N. Slijkhuis, M. Towers, M. Mirzaian, S.A. Korteland, B. Heijs, K. van Gaalen, I. Nieuwenhuizen, A. Nigg, K. van der Heiden, Y.B. de Rijke, A. van der Lugt, E.J. G. Sijbrands, E. Claude, G. van Soest, Identifying lipid traces of atherogenic mechanisms in human carotid plaque, Atherosclerosis 385 (2023) 117340, https://doi.org/10.1016/j.atherosclerosis.2023.117340.